



UNIVERSITY
OF TRENTO

DEPARTMENT OF INFORMATION AND COMMUNICATION TECHNOLOGY

38050 Povo – Trento (Italy), Via Sommarive 14
<http://www.dit.unitn.it>

A MICROWAVE IMAGING METHOD FOR NDE/NDT BASED ON THE
SMW TECHNIQUE FOR THE ELECTROMAGNETIC FIELD PREDICTION

Andrea Massa, Matteo Pastorino, Andrea Rosani, Manuel Benedetti

August 2004

Technical Report [DIT-04-073](#)

A Microwave Imaging Method for NDE/NDT based on the SMW Technique for the Electromagnetic Field Prediction

A. Massa,¹ M. Pastorino,² A. Rosani,¹ and M. Benedetti¹

¹ Department of Information and Communication Technologies, University of Trento
Via Sommarive 14, I-38050 Trento, Italy
Phone: +39 0461882057, Fax: +39 0461882093, E-mail: andrea.massa@ing.unitn.it

² Department of Biophysical and Electronic Engineering, University of Genoa
Via Opera Pia 11A, 16145, Genova, Italy
Phone: +39 010 3532242, Fax: +39 0103532245, E-mail: pastorino@dibe.unige.it

Abstract – *In the framework of NDE/NDT, this paper presents an innovative microwave diagnostic approach based on the use of the SMW inversion procedure for the electric field prediction. Starting from the integral form of inverse scattering equations, the problem of determining the presence of an unknown defect in a known host domain is recast into an optimization one by defining a suitable cost function and reducing the problem unknowns only to the flaw “descriptors”. By considering an effective inversion technique based on the SMW formula, the estimation of the secondary unknowns (namely, the electric field distributions) is performed in a cost-effective way. Selected numerical results are presented to validate the approach showing current potentialities and limitations. For completeness, an application to civil engineering is also reported.*

Keywords: *Imaging Systems, Imaging Processing, Genetic Algorithms, Nondestructive testing, SMW Inversion Method.*

I. INTRODUCTION

Noninvasive diagnostics methods based on microwaves have become more and more important in various applications, including industrial testing and evaluation, ranging from civil engineering to geophysical monitoring and biomedical analysis.[1]-[3] Between existing and emerging methodologies, imaging techniques are assuming particular relevance for the inspection of dielectric materials. In this framework, microwave imaging techniques based on the inverse scattering theory, starting from the discretized form of Fredholm equations [4], (i.e., the *data* and *state equation* governing the relation among the scattering potential, the total electric field inside the body, and the scattered electric field at the receivers) generally reformulate the arising problem in an optimization one where a suitably defined cost function is constructed (often arbitrarily) and successively minimized in order to estimate a map of the dielectric properties of the region under test. Toward this end, Caorsi *et al.* proposed in [5]-[7] the application of global optimization approaches [8][9], and, in particular, the use of a hybrid-coded genetic algorithm (GA) [10].

However, due to the large amount of problem unknowns, the main drawback of such very appealing methods is the high computational burden, which strongly increases along with the increasing of the spatial resolution accuracy. The continuous increasing in the computational power of new computers and the fully exploitation of the parallel nature of GA procedure could strongly limit this problem, but certainly a pixel representation of the cross section of an unknown complex object still represents a hard task. However, as far as the application to NDT/NDE problem is concerned, such a redundant information is not needed since the *object* to be detected is only a *defect* in an otherwise known object. The arising inverse scattering problem

is notably simplified as well as the dimension of the search space, thus allowing an effective use of a GA-based strategy. In this framework, Caorsi et al. recently proposed a customized approach [11] and a successive extension [12][13], which demonstrated their effectiveness in dealing with two-dimensional geometries. A further refinement of this method is presented in this paper. The proposed improvement is aimed at considerably increase the convergence speed of the algorithm by computing in a fast and more effective way the induced electromagnetic field. Moreover, such an approach avoids the coding of the secondary unknowns in the arising chromosome.

The paper is organized as follows. After the problem description, the mathematical formulation (Sec. II) of the approach will be described by focusing on the numerical procedure for the computation of the induced electric field distribution. Then, a set of selected numerical results will be shown (Sec. III). A preliminary assessment will be performed by considering reference scenarios. Then, the validation will be extended to more complex environments modeling realistic civil engineering test cases. Finally, some conclusions will follow (Sec. IV).

II. MATHEMATICAL FORMULATION

Let us consider the geometry shown in Figure 1. An unknown defect (yellow area) lies in a known host medium (red area) illuminated by a set of V TM unit plane waves, E_{inc}^v , $v=1, \dots, V$. The test sample (formally the *investigation domain*) is assumed to be of cylindrical shape, as in the case of a cement concrete or a column. It is surrounded by a circular arrangement of probing antennas located at M positions (x_m, y_m) , $m=1, \dots, M$ and forming a microwave scanner. Starting from the knowledge of the scattered field $E_{scatt}^v(x_m, y_m)$, $m=1, \dots, M$, $v=1, \dots, V$ collected by the probing antennas, and of the incident field $E_{inc}^v(x_n, y_n)$ $n=1, \dots, N$, $v=1, \dots, V$ measured at N positions in the investigation domain, the reconstruction procedure is aimed at finding the unknown descriptors of the crack assumed to be a homogeneous rectangle (i.e., the centre of mass (x_0, y_0) , the orientation α_c and the occupation rectangle defined by its dimensions L_c and W_c)

$$\bar{f}_{crack} = \{L_c, W_c, \alpha_c, x_0, y_0\} \quad (1)$$

and the electric field distribution for the flaw configuration $\bar{f}_{field} = \{E_{tot}^v(x_n, y_n), v=1, \dots, V; n=1, \dots, N\}$, by minimizing the following cost function, Φ

$$\Phi(\bar{f}) = \Phi_{Data}(\bar{f}) + \Phi_{State}(\bar{f}) \quad (2)$$

where

$$\Phi_{Data}(\bar{f}) = \frac{\sum_{v=1}^V \sum_{m=1}^M |E_{scatt}^v(x_m, y_m) - \mathfrak{S}_{Data}^m\{\bar{f}\}|^2}{\sum_{v=1}^V \sum_{m=1}^M |E_{scatt}^v(x_m, y_m)|^2}$$

and

$$\Phi_{State}(\bar{f}) = \frac{\sum_{v=1}^V \sum_{n=1}^N |E_{inc}^v(x_n, y_n) - \mathfrak{S}_{State}^n\{\bar{f}\}|^2}{\sum_{v=1}^V \sum_{n=1}^N |E_{inc}^v(x_n, y_n)|^2}.$$

where $\bar{f} = \{\bar{f}_{crack}, \bar{f}_{field}\}$. As in [13] and [14], the basic idea of the approach is the definition of a succession $\{\bar{f}_k\}$, $k = 1, \dots, K$ of trial configurations, which converges to the minimum of (2) according to a GA-based strategy.

However, in order to reduce the search space and to improve the reconstruction accuracy of the approach, it could be profitable to use the relation between the induced electric field and the defect configuration, which in matrix form turns out to be expressed as follows

$$[E_{tot}^v] = [\Psi]^{-1} [E_{inc}^v] \quad (3)$$

where $[\Psi]^{-1} = \{[I] - [G][\tau]\}$ and τ indicates the mapping of the crack descriptors into the object function distribution inside the discretized-scatterer geometry. The matrix $[G]$ is the discretized representation of the free-space Green's function for two-dimensional geometries [1]. The solution of the arising "direct" problem generally requires a time-consuming process (that strongly reduces the possibility of an on-line implementation). A more effective solution is the use of the Sherman-Morrison-Woodbury (SMW) formula [15]. Starting from the computation (performed once and off-line for any host-medium configuration) of the "state" operator $[\Psi_{un}]^{-1}$ for the unperturbed geometry

$$[E_{tot(cf)}^v] = [\Psi_{un}]^{-1} [E_{inc}^v] \quad (4)$$

$E_{tot(cf)}^v$ being the array related to the electric field of the unperturbed geometry and characterized by an object function distribution $\tau_{host}(x_n, y_n)$, it is possible to compute (3) according to the following relation [15]:

$$[\Psi]^{-1} = [\Psi_{un}]^{-1} + [\Psi_{un}]^{-1} [U] \{[I] - [V]^T [\Psi_{un}]^{-1} [U]\}^{-1} [V]^T [\Psi_{un}]^{-1} \quad (5)$$

where $[U]$ is given by the non-null columns of the difference matrix, $\{[\Psi_{un}]^{-1} - [\Psi]^{-1}\}$, and $[V]$ is computed according to the numerical procedure described in [16].

III. NUMERICAL VALIDATION

In order to assess the effectiveness of the SMW-based approach (SMWA), several numerical experiments have been carried out and representative results will be reported in the following.

Preliminary, the validation of the proposed approach is performed by considering a reference scenario and different situations for which state-of-the-art methods have been already checked. In particular, for comparison purposes, the obtained results will be evaluated with the estimates from a reference approach, in the following named IGA (Inhomogeneous Green Function based Approach) [12]. The two-dimensional scenario is characterized by an unknown void defect lying in a square losses homogeneous host medium ($L_{host} = 0.8 \lambda$ in side and characterized by $\epsilon_R^{host} = 2.0$). Such an investigation domain is illuminated at $V = 4$ orthogonal angular positions and the scattered data are collected at $M = 50$ measurement points. The achieved results have been evaluated in terms of localization error.

$$\delta_c = \frac{\sqrt{(x_0 - \hat{x}_0)^2 + (y_0 - \hat{y}_0)^2}}{d_{max}} \times 100 \quad (6)$$

and area-estimation error

$$\delta_A = \frac{|A_c - \hat{A}_c|}{A_c} \times 100 \quad (7)$$

where $A_c = L_c \times W_c$, d_{\max} is the maximum linear dimension of the investigation domain and the superscript \wedge differentiates actual from estimated values.

Since the statistical nature of the minimization procedure [9][10], each simulation has been repeated 10 times and the results averaged. The average values of the error figures will be shown in a color-level representation.

As far as the first test case is concerned, the area of the void crack, centered in $(0.15\lambda, 0.1\lambda)$ has been changed between $2.5 \times 10^{-3} \lambda^2$ and $2.5 \times 10^{-1} \lambda^2$, by considering various environment conditions characterized by different signal-to-noise ratios (SNR) from 2.5 to 30.0 dB (modeling the electromagnetic interferences and experimental errors). As can be observed (Figs. 2(a)-(b)), the SMW-based approach (as well as the reference approach) is able to correctly localize the defect with an average localization error lower than 4%. For small cracks ($A_c < 5 \times 10^{-2} \lambda^2$) and high level of noise, the localization accuracy of the three approaches reduces. However, the maximum localization error does not increase over 42%. Concerning the estimation of the area of the defect (Figs. 3(a)-(b)), generally SMWA outperforms on average the IGA procedure ($av\{\delta_A\}_{SMWA} \cong 14\%$, $av\{\delta_A\}_{IGA} \cong 15\%$). In particular, the reconstruction error is lower than 30% in the following range $0.01\lambda^2 < A_c < 0.18\lambda^2$. As expected, the proposed approach optimally predicts the induced electric field distribution. On an average, the error turns out to be equal to $av\{\Delta E^{tot}\}_{SMWA} \cong 6.0\%$ (Fig. 4(b)). However, when the dimension of the defect is greater than $0.20\lambda^2$, then value of the field error increases since the actual and crack-free configurations significantly differ and the effectiveness of the SMW procedure reduces.

The second test case refers to a lossy reference scenario whose conductivity ranges from $0.0S/m$ to $1.0S/m$ and the actual defect is a square with an area equal to $A_c = 0.08\lambda^2$ and centered at $x_0 = 0.26\lambda$ and $y_0 = 0.0\lambda$. As can be noticed (Fig. 5(b)), the SMWA correctly locates the defect in the investigation domain and the average value of the localization error turns out to be equal to $av\{\delta_c\}_{SMWA} \cong 3.22\%$. Similar results are achieved by using the IGA procedure (Fig. 5(a)). The two methods confirm their effectiveness also in estimating the dimensions of the defect (Figs. 6(a)-(b)). However, the effectiveness of the proposed approaches reduce with respect to the losses condition and the average error turns out to be $av\{\delta_c\}_{SMWA} \cong 15.6\%$. Once more and as expected, the SMWA shows its effectiveness in predicting the electric field with errors lower than 3.4% in any environment conditions (Fig. 7(b)).

The second part of the validation deals with more complex scenarios related to the civil engineering framework [17]. Figure 8 shows the geometries of the various test cases. The investigation domain is supposed to be a square cylinder $L_d = 4.167\lambda_0$ -sided and $M = 50$ measurement points have been placed in a circular observation domain $2.83\lambda_0$ in radius by considering the same illumination conditions of the previous cases. Moreover, the geometry indicated as ‘‘Structure Type 1’’ (Fig. 8(a)) models a homogeneous cement paste characterized by $\epsilon_R^{host} = 2.37$ and $\sigma^{host} = 5.7 \times 10^{-4} S/m$. The second one (‘‘Structure Type 2’’ – Fig. 8(b)) considers the presence of a squared load bearing ($0.42\lambda_0$ -sided) in the center of the structure ($\epsilon_R^{steel} = 1.0$, $\sigma^{steel} = 1.1 \times 10^6 S/m$). The ‘‘Structure Type 3’’ (Fig. 8(c)) is composed by a load bearing beam with 4 steel bars and represents a ‘‘reinforced concrete’’ structure. The square bars are $0.31\lambda_0$ -sided and the distance from the border of the pillar is equal to $0.52\lambda_0$.

As far as the geometry shown in Fig. 8(a), both the SMWA and the IGA techniques perform the localization of the defect with a maximum error $\{\delta_c\} < 10\%$ (Fig 9(a)) when the area of the crack satisfies the following relation $A_c > 0.22 \times 10^{-3} \lambda_0^2$. However, the SMWA overcomes the results of the reference approach in estimating the area of the crack. The error turns out to be $\{\delta_a\} < 25\%$ in the all range of variation (Fig 9(b)).

In dealing with an inhomogeneous medium (Fig. 8(b), “Structure Type 2”), the crack is again localized with an adequate accuracy and the average error is equal to $av_{A_c/\lambda^2=0.01, \dots, 0.88} \{\delta_c\} = 22\%$ both in the case of SMWA and IGA (Fig. 10(a)). On the other hand, the error in estimating the defect is considerably reduced using the new approach with error values $\{\delta_a\} < 35\%$ ($av_{A_c/\lambda^2=0.01, \dots, 0.88} \{\delta_a\} = 47\%$ for the IGA approach) (Fig. 10(b)).

Finally, “Structure Type 3” (Fig. 8(c)) points out that the presence of a set of four steels bars significantly affects the performances of the IGA method and seems to indicate better reconstruction capabilities of the SMWA method. As can be observed (Fig. 11(a)-(b)), the results obtained with the SMWA approach overcome both in localization and crack dimensioning that of the IGA approach. More in detail, $av_{A_c/\lambda^2=0.01, \dots, 0.88} \{\delta_c\} = 10\%$ and $\{\delta_a\} < 38\%$.

IV CONCLUSIONS AND FUTURE DEVELOPMENTS

In conclusion, a microwave imaging approach based on the solution of the inverse scattering equations has been proposed by considering an effective use of the *a-priori* information of the scenario under test and a non-computationally expensive numerical procedure for the field prediction. Selected numerical simulation with particular reference to realistic structures in the framework of civil engineering have been considered and demonstrated a significant effectiveness of the proposed approach in the defect retrieval.

Future developments and researches will be aimed at further exploit the *a-priori* information of the scenario under test in order to allow an extension of the proposed procedure to three-dimensional geometries.

REFERENCES

- [1] R. Zoughi, *Microwave Testing and Evaluation*. Kluwer Academic Publishers, The Netherlands, 2000
- [2] G.C. Giakos, M. Pastorino, F. Russo, S. Chowdhury, N. Shah, and W. Davros, "Noninvasive imaging for the new century", *IEEE Instrumentation and Measurement Magazine*, vol. 2, pp. 32-35, 1999.
- [3] E. C. Fear, P. M. Meaney, and M. A. Stuchly, "Microwaves for breast cancer detection," *IEEE Potentials*, vol. 22, pp. 12-18, 2003.
- [4] D. S. Jones, *The Theory of Electromagnetism*. Oxford, U.K.: Pergamon Press, 1964.
- [5] M. Pastorino, A. Massa and S. Caorsi, "A microwave inverse scattering technique for image reconstruction based on a genetic algorithm," *IEEE Transactions on Instrumentation and Measurement*, vol. 49, pp. 573-578, June 2000.
- [6] A. Massa, "Genetic Algorithm (GA) Based Techniques for 2D Microwave Inverse Scattering," in *Recent Research Developments in Microwave Theory and Techniques* (Special Issue on *Microwave Non-Destructive Evaluation and Imaging*), Ed. M. Pastorino, Transworld Research Network Press, Trivandrum, India, pp. 193-218, 2002.
- [7] M. Pastorino, A. Massa, and S. Caorsi, "Reconstruction algorithms for electromagnetic imaging," *Proc. IMTC 2002*, Anchorage, Alaska, USA, pp. 1695-1799, May 21-23, 2002.
- [8] D. E. Goldberg, *Genetic Algorithms in Search, Optimization, and Machine Learning*. Addison-Wesley, Reading, MA, USA, 1989.
- [9] J.M. Johnson and Y. Rahmat-Samii, "Genetic algorithms in engineering electromagnetics," *IEEE Transactions on Antennas and Propagation Magazine*, vol. 39, pp. 7-26, 1997.
- [10] S. Caorsi, A. Massa, and M. Pastorino, "A Computational Technique Based on a Real Coded Genetic Algorithm for Microwave Imaging Purposes", *IEEE Transactions on Geoscience and Remote Sensing* - Special Issue on "Computational Wave Issues in Remote Sensing, Imaging and Target Identification," vol. 38, pp. 1697-1708, 2000.
- [11] M. Pastorino, A. Massa, and S. Caorsi, "A global optimization technique for microwave nondestructive evaluation," *IEEE Transactions on Instrumentation and Measurement*, vol. 51, pp. 666-673, 2002.
- [12] S. Caorsi, A. Massa, M. Pastorino, A. Randazzo, and A. Rosani, "A reconstruction procedure for microwave nondestructive evaluation based on a numerically computed Green's function," *Proc. IMTC 2003*, Vail, Colorado, USA, pp. 669-674, May 20-22, 2003.
- [13] S. Caorsi, A. Massa, M. Pastorino, and M. Donelli, "Improved microwave imaging procedure for non-destructive evaluations of two-dimensional structures," *IEEE Transactions on Antennas and Propagation*, vol. 52, no. 6, pp. 1386-1397, June 2004.
- [14] S. Caorsi, A. Massa, M. Pastorino, "A crack identification microwave procedure based on a genetic algorithm for nondestructive testing," *IEEE Transactions on Antennas and Propagation*, vol. 49, pp. 1812-1820, 2001.
- [15] E. Yip and B. Tomas, "Obtaining Scattering Solution for Perturbed Geometries and Materials from Moment Method Solutions", *ACES Journal*, pp. 95-118, 1988.
- [16] S. Caorsi, A. Massa, and M. Pastorino, "Application of the UMoM for the computation of the scattering by dielectrics with weakly nonlinear layers," *ACES Journal* - Special Issue on "Advances in the Application of the Moment of Methods to Electromagnetic Radiation and Scattering Problems," vol. 10, pp. 139-145, 1995.
- [17] W. H. Hayt Jr., J. A. Buck, *Engineering Electromagnetics*, New York, USA, McGraw-Hill, 2001

FIGURE CAPTIONS

- Figure 1.** NDE/NDT problem geometry.
- Figure 2.** Test Case No 1. – Localization Error: (a) IGA and (b) SMWA.
- Figure 3.** Test Case No 1. – Area Estimation Error: (a) IGA and (b) SMWA.
- Figure 4.** Test Case No 1. – Field Estimation Error: (a) IGA and (b) SMWA.
- Figure 5.** Test Case No 2. - Localization Error: (a) IGA and (b) SMWA.
- Figure 6.** Test Case No 2. – Area Estimation Error: (a) IGA and (b) SMWA.
- Figure 7.** Test Case No 2. – Field Estimation Error: (a) IGA and (b) SMWA.
- Figure 8.** Models of civil structures: (a) “Type 1”, (b) “Type 2”, and (c) “Type 3”.
- Figure 9.** Structure “Type 1” – Error Figures: (a) localization error and (b) area estimation error.
- Figure 10.** Structure “Type 2” – Error Figures: (a) localization error and (b) area estimation error.
- Figure 11.** Structure “Type 3” – Error Figures: (a) localization error and (b) area estimation error.

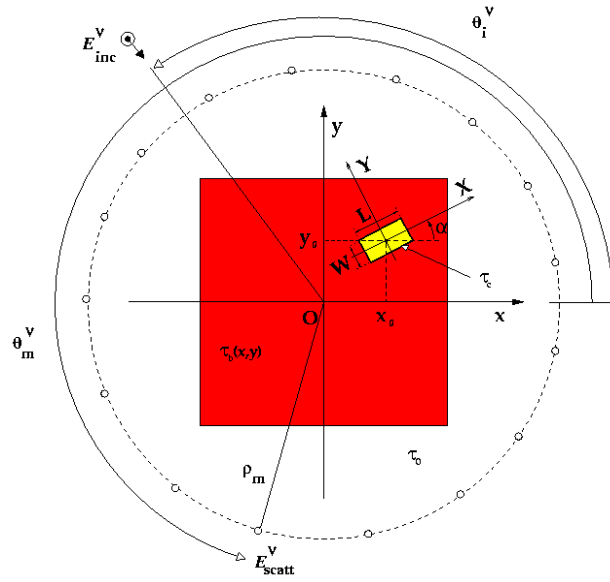
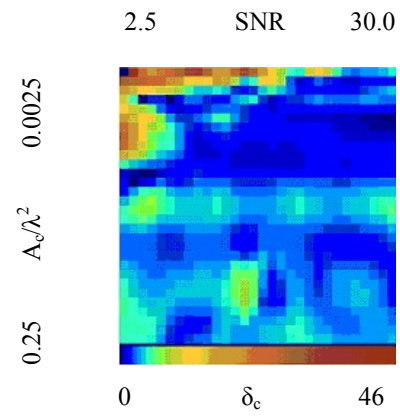
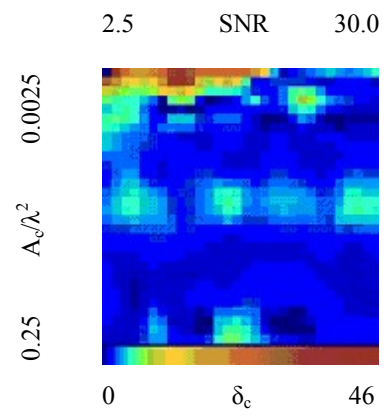


Fig. 1 – A. Massa *et al.*, “A Microwave Imaging Method for NDE/NDT...”

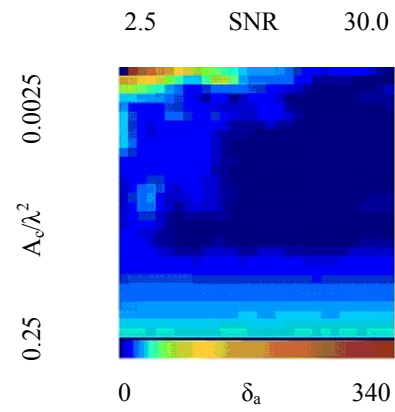


(a)

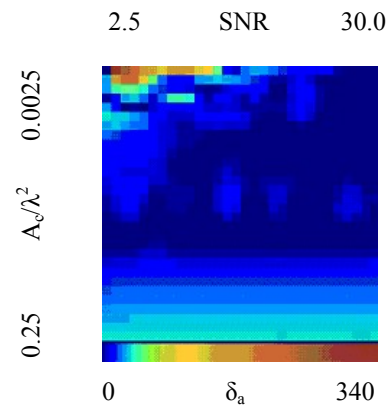


(b)

Fig. 2 – A. Massa *et al.*, “A Microwave Imaging Method for NDE/NDT...”

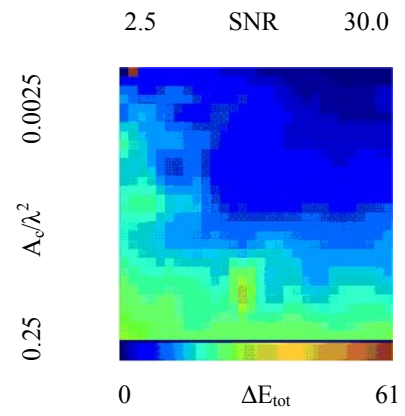


(a)

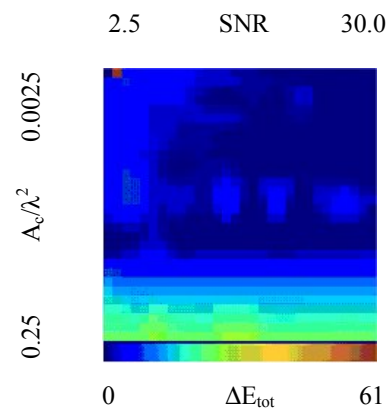


(b)

Fig. 3 – A. Massa *et al.*, “A Microwave Imaging Method for NDE/NDT...”

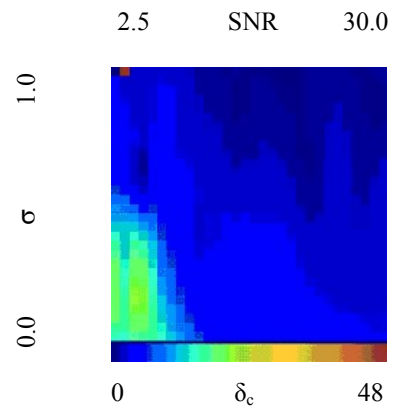


(a)

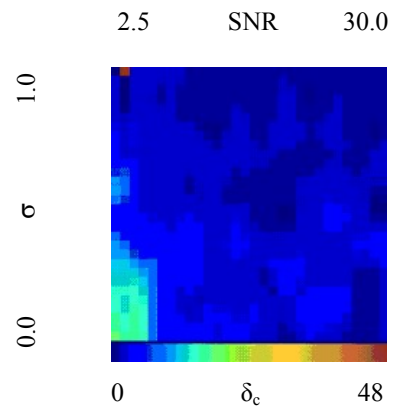


(b)

Fig. 4 – A. Massa *et al.*, “A Microwave Imaging Method for NDE/NDT...”

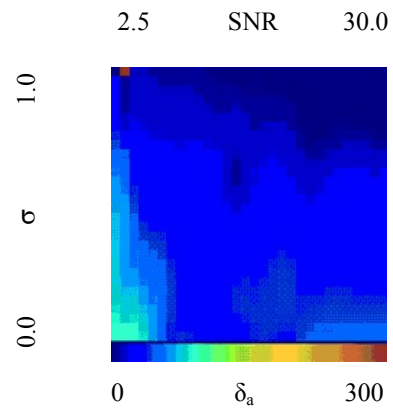


(a)

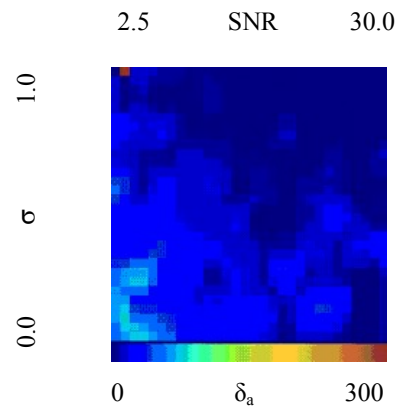


(b)

Fig. 5 – A. Massa *et al.*, “A Microwave Imaging Method for NDE/NDT...”

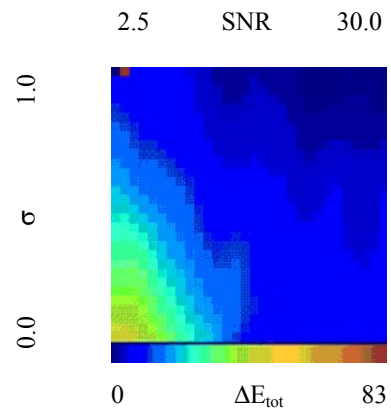


(a)

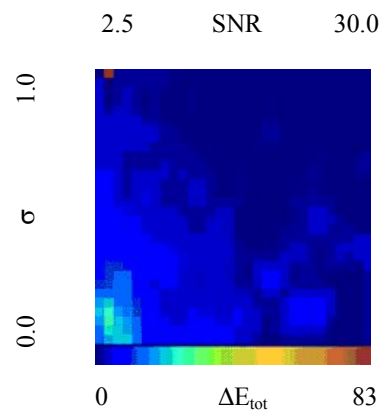


(b)

Fig. 6 – A. Massa *et al.*, “A Microwave Imaging Method for NDE/NDT...”



(a)



(b)

Fig. 7 – A. Massa *et al.*, “A Microwave Imaging Method for NDE/NDT...”

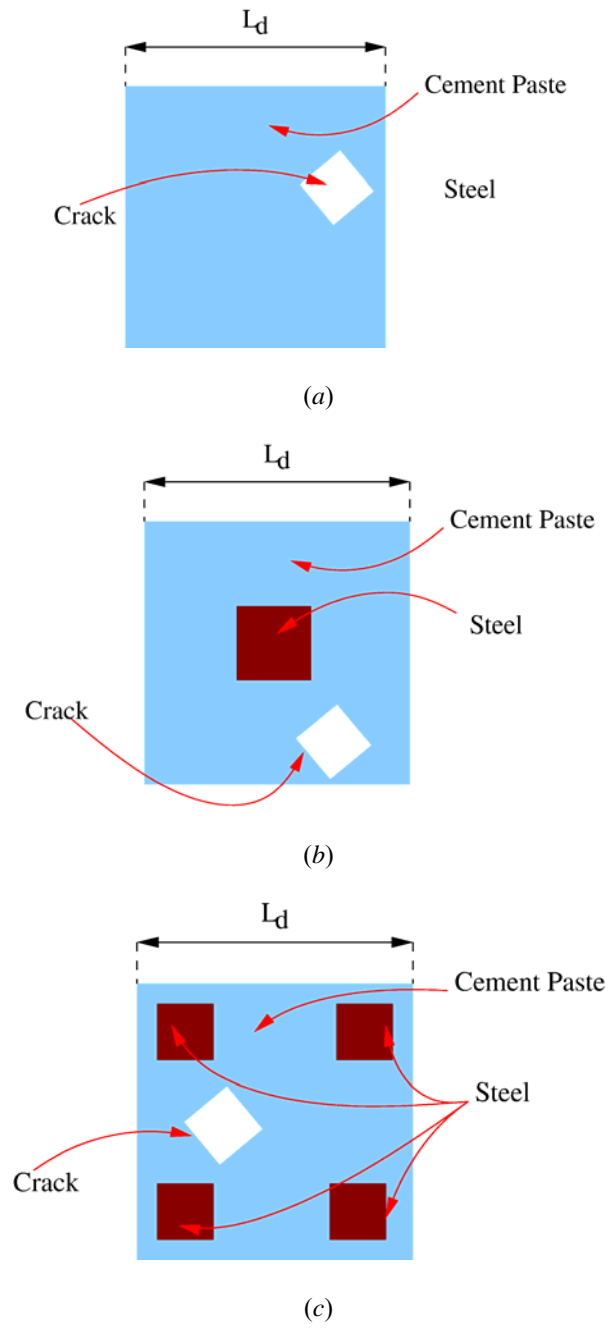
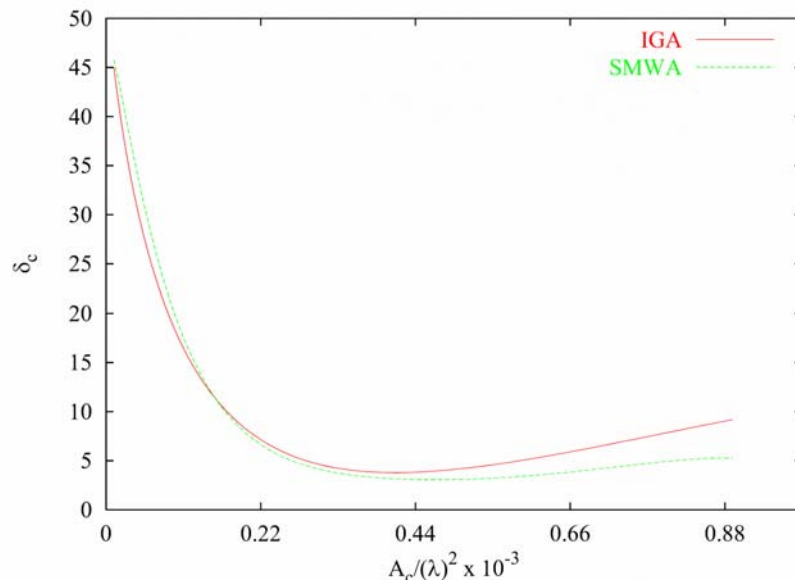
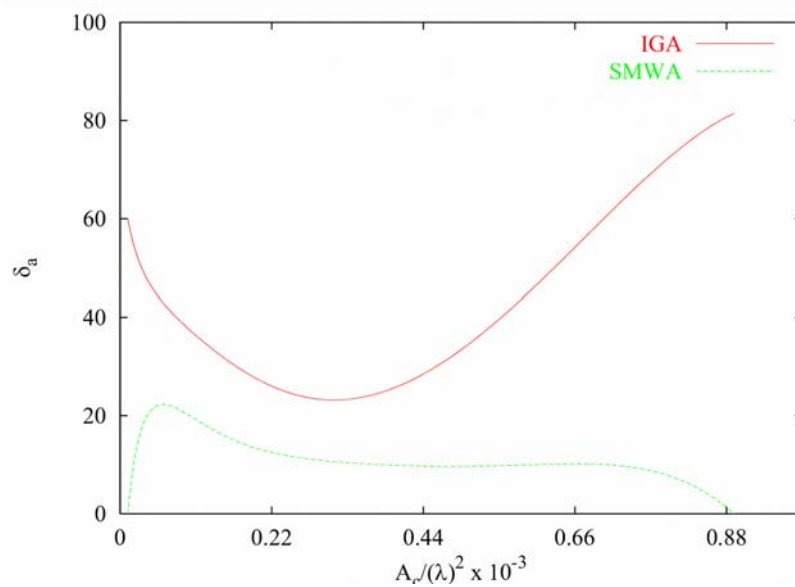


Fig. 8 – A. Massa *et al.*, “A Microwave Imaging Method for NDE/NDT...”

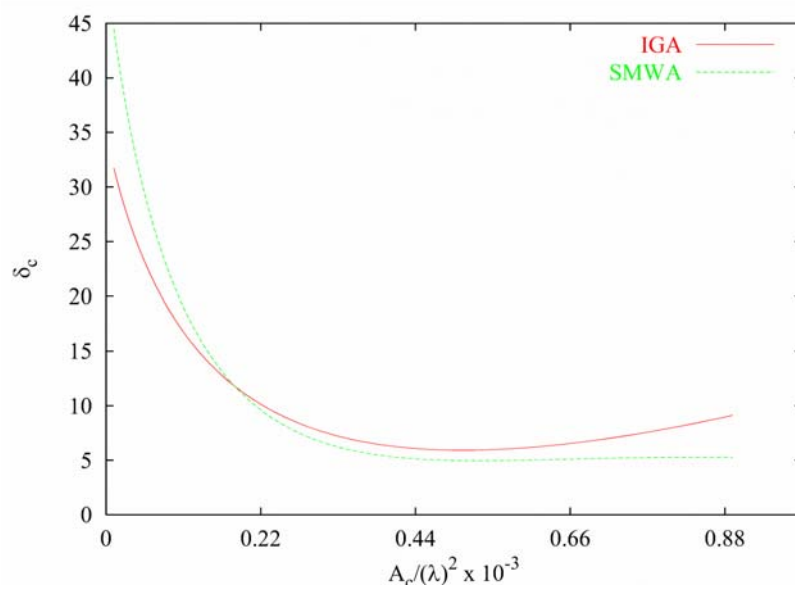


(a)

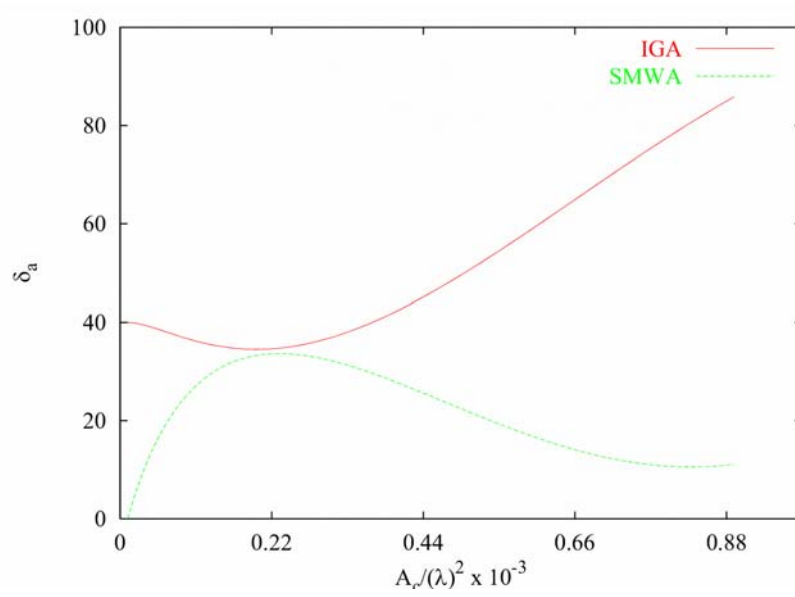


(b)

Fig. 9 – A. Massa *et al.*, “A Microwave Imaging Method for NDE/NDT...”

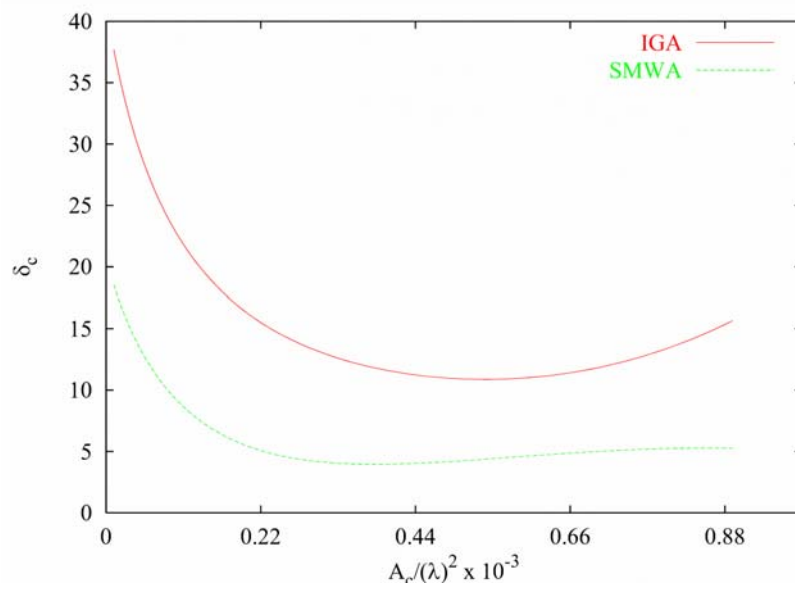


(a)

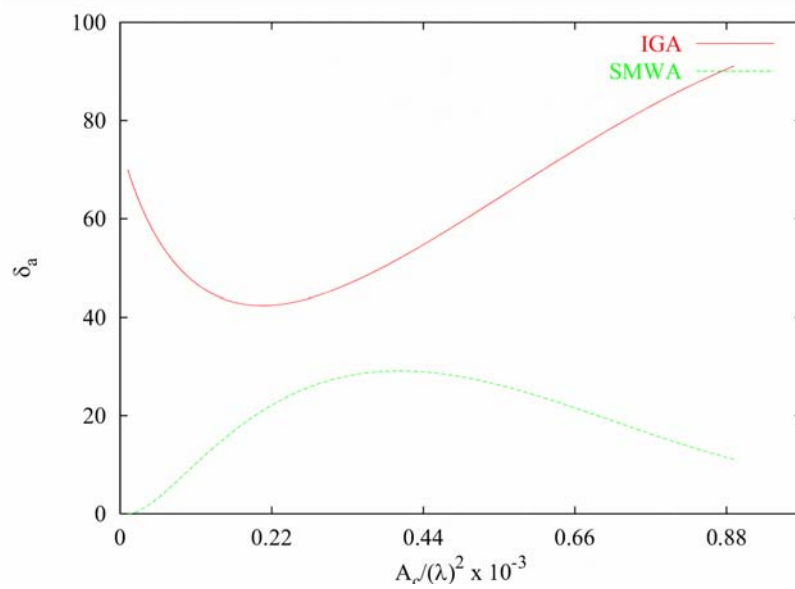


(b)

Fig. 10 – A. Massa *et al.*, “A Microwave Imaging Method for NDE/NDT...”



(a)



(b)

Fig. 11 – A. Massa *et al.*, “A Microwave Imaging Method for NDE/NDT...”